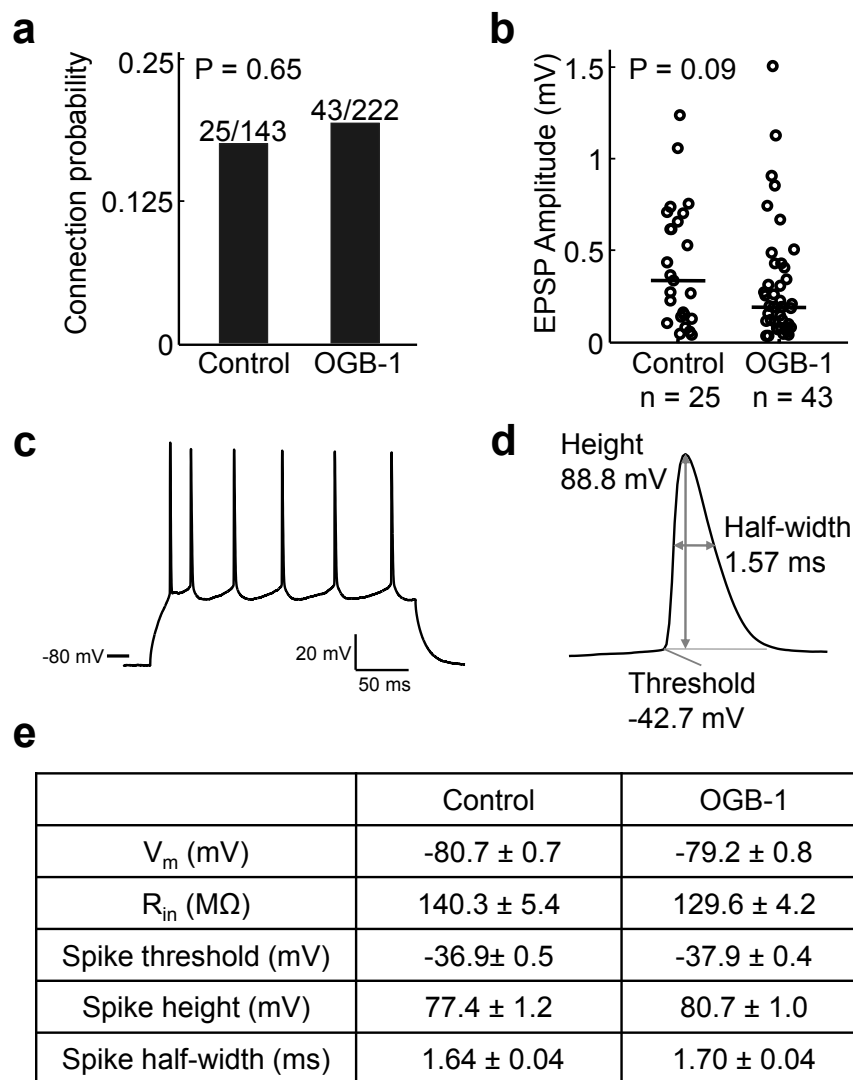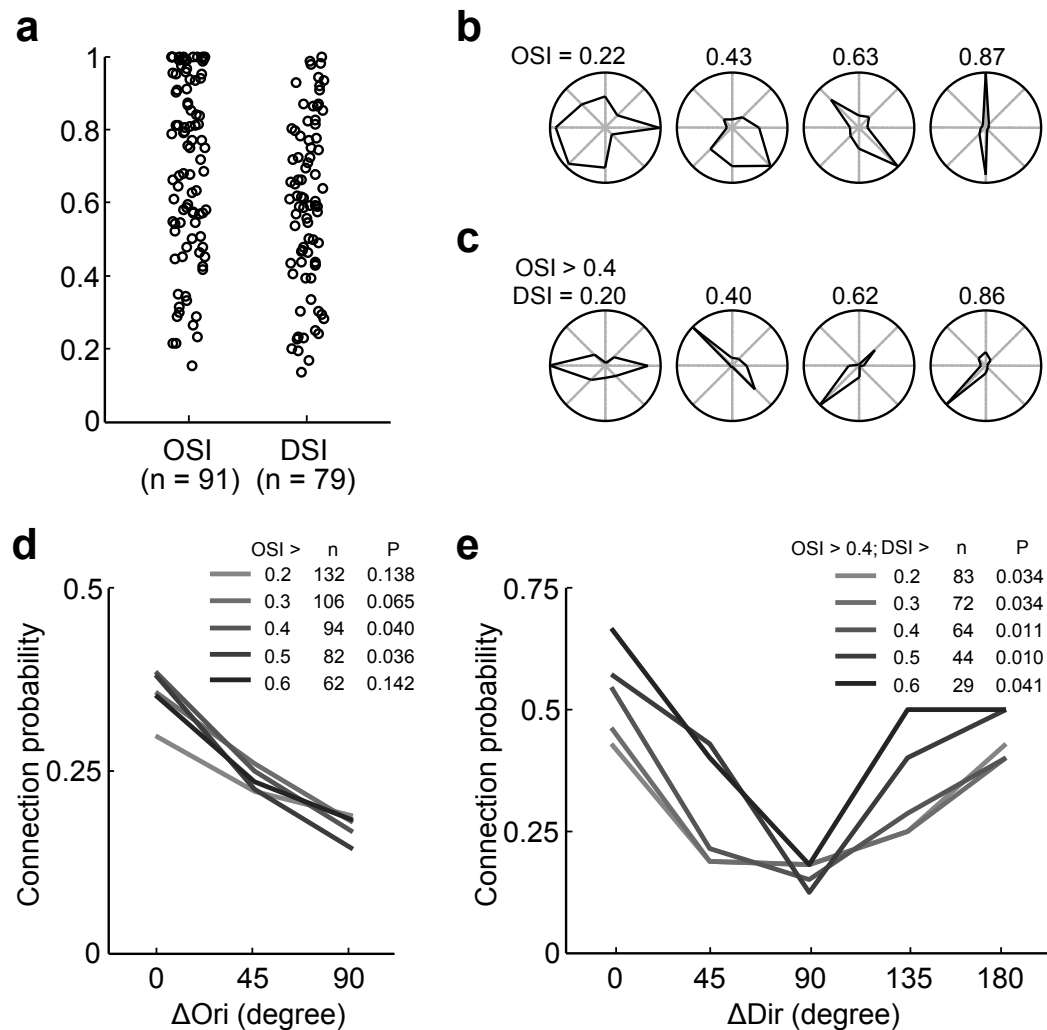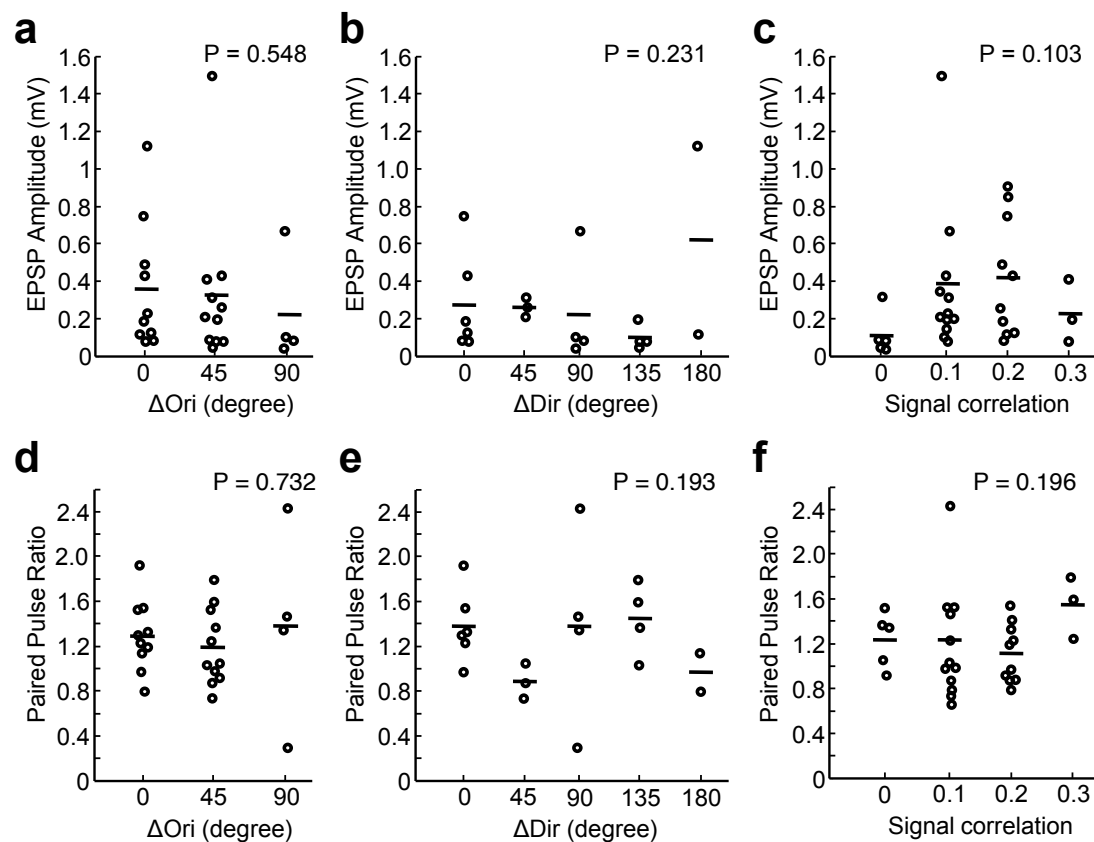Supplementary Figure 1. Method for registering *in vivo* and *in vitro* image stacks. a, In the first step, three pairs of corresponding points were identified in the *in vivo* and *in vitro* stacks. Red fluorescent bead injections allowed fast selection of the slice containing the imaged volume and also helped in giving the experimenter an idea of the orientations of structures in the stacks. In this example, three pairs of astrocytes outlined by red, blue and yellow circles alongside the beads were picked. Depths of the images from the top of the *in vivo* and *in vitro* stacks (which correspond approximately to depths from cortical and slice surface, respectively) are shown at left bottom corner. **b**, After picking the first three pairs of points, the stacks were rotated, such that the planes containing the three pairs of points (outlined by circles of the same color) in each stack became parallel to the xy-plane. The *in vitro* stack was further transformed in 2D to register it to the plane from the in vivo stack (upper panel) (see Methods). The stacks then became roughly registered in 2D, but not along the z-axis. To find the affine transformation needed for registering the *in vivo* stack to the *in vitro* stack a fourth pair of corresponding points (outlined by violet circles in lower panel) were picked from another plane. **c,d**, With four pairs of corresponding points known, the affine transformation was found and applied to the *in vivo* stack to bring it in register with the *in vitro* stack, hence allowing matching of cells. Scale bars in all panels: 30 μm.

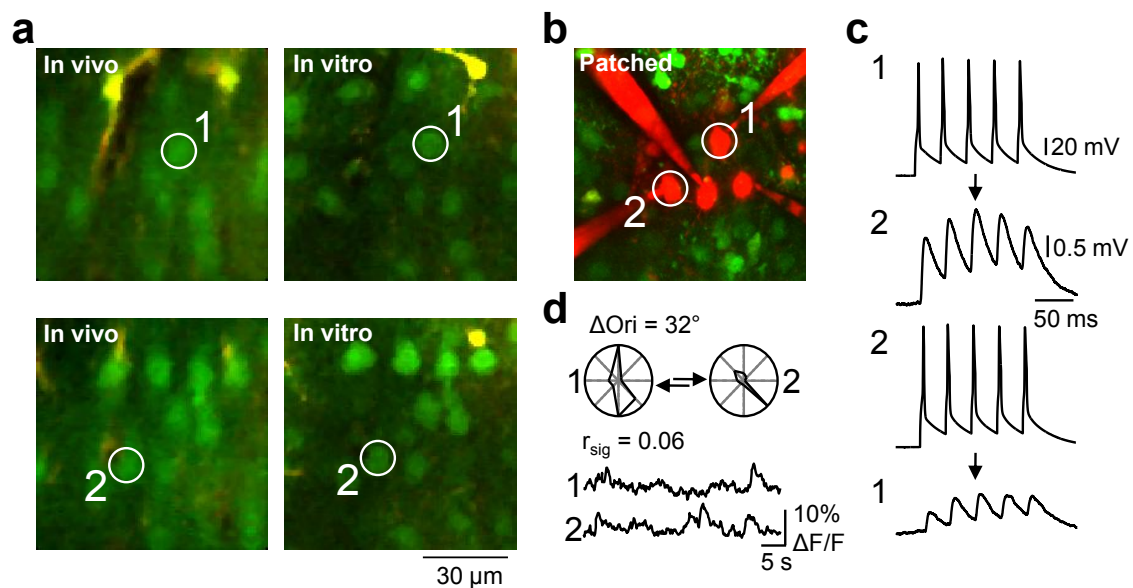|	Control	OGB-1
V_m (mV)	-80.7 ± 0.7	-79.2 ± 0.8
R_{in} (MΩ)	140.3 ± 5.4	129.6 ± 4.2
Spike threshold (mV)	-36.9± 0.5	-37.9 ± 0.4
Spike height (mV)	77.4 ± 1.2	80.7 ± 1.0
Spike half-width (ms)	1.64 ± 0.04	1.70 ± 0.04

Supplementary Figure 2. Comparison of connection probability, synaptic strength and electrophysiological properties of neurons in slices obtained from visual cortex injected with OGB-1 AM and naive age-matched visual cortex. a, Connection probability was similar in OGB-1-labeled tissue and control (non-labeled) slices (25/143 vs 43/222, P = 0.65, Chi-square test). **b,** Comparison of synaptic strength: median EPSP amplitude (black line) was lower in OGB-1-labeled slices although the difference was not significant (P = 0.09, rank sum test). While this could potentially have caused more weak synapses to escape detection, this was unlikely as indistinguishable connection rates were observed in OGB-1 and control slices. **c, d,** Firing pattern (during 500 ms of 300 pA current injection) and spike parameters from a sample cell, typical of pyramidal neurons. **e,** Electrophysiological properties of neurons patched in OGB-1 and control slices and included in connectivity analysis were similar. Numbers are mean ± SEM.

Supplementary Figure 3. Main findings do not depend on criteria for orientation and direction selectivity. a, The distribution OSI of all neurons that were responsive to grating stimuli, and the distribution of DSI of all neurons that were responsive to grating stimuli (with OSI > 0.4). **b**, Polar plots of sample neurons with different OSI and DSI values. Neurons with lower OSI values responded to a broader range of grating orientations, whereas neurons with high OSI values showed narrow tuning. **c**, Similarly, neurons with higher DSI values exhibited clearer preference to one of the directions of the preferred grating orientation. **d**, Varying the criterion for orientation selectivity from 0.2 to 0.6 did not change the relationship between connection probability and similarity of orientation preference. **e**, Varying the criterion for direction selectivity from 0.2 to 0.6 did not change the relationship between connection probability and similarity of orientation preference in direction selective pairs.
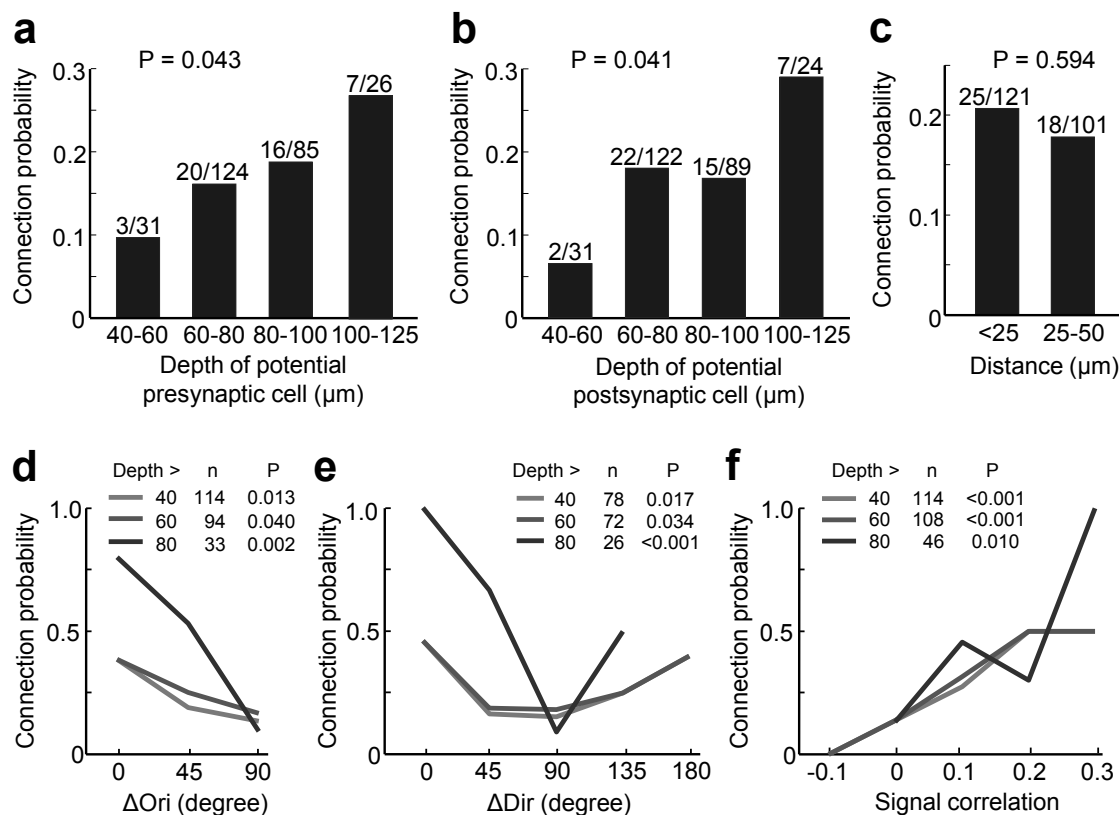
Supplementary Figure 4. Relationship between EPSP amplitude and paired-pulse ratio (PPR) and orientation preference, direction preference and signal correlation to natural movie. a and b, No significant difference between EPSP amplitudes of connections between pairs of different ΔOri was found among either orientation selective (P = 0.548, Kruskal-Wallis test), or direction selective connected pairs (P = 0.231, Kruskal-Wallis test). c, EPSP amplitudes were not found to change significantly with increase in signal correlation to natural movie (P = 0.103, Kruskal-Wallis test). d and e, There was no significant difference between PPRs of connections between pairs of different ΔOri among either orientation selective (P = 0.732, Kruskal-Wallis test), or direction selective connected pairs (P = 0.193, Kruskal-Wallis test). f, PPR did not vary significantly with signal correlation to natural movies (P = 0.196, Kruskal-Wallis test).

Supplementary Figure 5. Example of a pair of neurons with strong reciprocal connections.
a, *In vivo* and *in vitro* images of cell pair patched. The two pyramidal neurons were at different depths from the slice surface and hence two pairs of images are shown. White circles outline the positions of the cells. **b**, Maximum intensity projection of 30 optical planes (separated by 1 μm) of the cell pair patched and filled with Alexa 594. **c**, Average traces of presynaptic spikes and EPSPs recorded from the neurons. A strong connection (amplitude = 1.50 mV) was found from cell 1 to cell 2, and another connection (amplitude = 0.43 mV) was found from cell 2 to cell 1. **d**, Orientation tuning and average response traces of the cells to natural movie sequences. Despite presence of relatively strong connections they did not have similar orientation preferences (ΔOri = 32˚) or a high signal correlation (0.06).

Supplementary Figure 6. Dependence of connection probability on depth of neurons from slice surface and distance between neurons. a, **b**, Probability of finding connections increases significantly as the depth of either potential presynaptic neuron (P = 0.043, Cochran-Armitage test) or postsynaptic neuron (P = 0.041, Cochran-Armitage test) increases. **c**, Beyond 60 μm from slice surface, among neuronal pairs separated by less than 50 μm, no significant difference in connection probability was found among pairs separated by less than or more than 25 μm (P = 0.594, Chi-square test). **d-f**, inclusion of neuronal pairs closer to slice surface increases false negative rates of connection detection, but did not change the main results. Increasing the depth criterion reduced sample number, but the significant dependence of connection probabilities on ΔOri, ΔDir and signal correlation was still maintained. In **e**, no connections were assayed between neuronal pairs that differ in preferred direction by 180° beyond 80 μm into the slice and hence one point on the plot is missing.